The behaviour of precast UHPC nodes for timber structures: A numerical study

A. Abdallah [a,*], M. Shahnewaz [b], C. Dickof [b], L. Tobber [a]

[a] University of British Columbia, Kelowna, Canada
[b] Fast+Epp, Vancouver, Canada
* Corresponding author: amr.abdallah@ubc.ca; amr.em.abdallah2017@gmail.com

Abstract:
Mass timber emerged over the last few decades as a reliable and sustainable structural material to meet the needs of growing urbanization, especially with the current surge in the frequency of natural disasters owing to global warming. In addition to reducing the carbon footprint of the building and aesthetic appearance, the use of mass timber also provides sufficient fire resistance through charring. However, the commonly used metallic connectors (e.g., at beam-column connections) may jeopardize the structure's integrity during fire, need additional costs for fireproofing, and have installation complexities. Therefore, the novel precast ultra-high-performance concrete (UHPC) was introduced, providing an aesthetic appearance, ease of installation and adequate fire resistance. This paper presents the details of constructing a finite-element model (FEM) for UHPC nodes, which was validated against experimental tests. This was followed by the finite-element analysis (FEA) of UHPC nodes with varying widths, depths, and shear spans of the corbels. The results indicated that the load-carrying capacity of the UHPC nodes (which all failed by flexural cracking) does not follow the conventional equation of flexural strength for concrete prisms. Therefore, a modified prediction equation was proposed to estimate the load capacity of UHPC nodes, which predicted the load capacity with reasonable accuracy.

Keywords:
Ultra high-performance concrete (UHPC), timber, corbel, beam-column joint, finite-element modelling

1. Introduction

Mass timber structural systems have become popular, particularly for gravity load-resisting frames (GLRFs), due to the incorporation of a sustainable and cost-effective material. An example of such a system is the 10-storey mass timber *The Hive* (formerly Keith Drive) office building in Vancouver [1], where steel connections were used to connect the glulam columns and a combination of steel and aluminum beam-to-column connectors.

Such metallic connections impose high costs and practical challenges due to installation complexities and the need for fireproofing to satisfy the required fire rating of the structure. As an alternative, the authors proposed precast ultra-high-performance concrete (UHPC) nodes [2], offering adequate fire resistance, ease of installation, and reduced cost.

To further validate the structural response of such novel nodes, this paper aims to validate a three-dimensional (3D) finite-element model (FEM) using ABAQUS software against experimental results of UHPC nodes and prisms [2] to conduct a parametric study to explore the effects of different parameters on the performance of such nodes. Based on the numerical analysis results, an analytical model is proposed to predict the load-carrying capacity of the nodes.

2. Details of the numerical model and validation

The UHPC elements were modelled using the C3D8R solid elements in ABAQUS. The load was applied through the top surface, whereas the corbels were supported on 20-mm wide surfaces, with multi-point constraints (MPC) to reference points at the mid-length of each corbel to simulate the steel bar supports in the experimental tests. The loading was applied as a gradual vertical downward displacement on the loaded surface. A mesh size of 10 mm was used to provide accurate results without excessive computational complexity. Fig. 1 shows the FEM and associated boundary conditions.

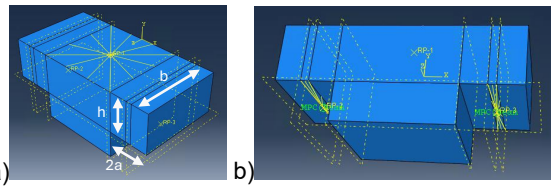

a) b)

Fig 1: Top boundary conditions (a); and bottom boundary conditions of the FEM (b).

Table 1: Modeling parameters for UHPC

Elastic properties				
Modulus of elasticity (MPa)			Poisson's ratio	
30,000			0.19	
Concrete damage plasticity (CDP) model parameters				
Dilation angle	eccentricity	fb0/fc0	K	Viscosity parameter
38°	0.1	1.1	0.667	0.0001

The concrete damage plasticity (CDP) model [3] was used to define the characteristics of UHPC, as listed in Tables 1 and 2. The CDP model in tension was verified using reverse analysis to simulate the load-

deflection response of the prisms tested for flexural strength [4].

Table 2: Concrete damage plasticity (CDP) model in compression and tension

Compression [5]		Tension [6]	
Yield strength (MPa)	Inelastic strain	Yield strength (MPa)	Cracking strain
f_c = 125	0	$f_{t,cr}$ = 0.7	0
f'_c = 130	$\varepsilon_{pl,peak}$ = 0.003	f_t = 9.3	$\varepsilon_{pl,t}$ = 0.0035
$f_{c,crush}$ = 40	$\varepsilon_{pl,crush}$ = 0.018	$f_{t,r}$ = 2	$\varepsilon_{pl,r}$ =0.03

Six FEMs were created following the geometry of the nodes tested by Abdallah et al. [2], as listed in Table 3. The results of FEM were compared against the experimental results in terms of load-deflection relationships and mode of failure.

Table 3: Properties of the UHPFRC node specimens.

Specimen ID	Lower column stub	Corbel		
		Width (mm)	thickness (mm)	length (mm)
A	Y	100	100	150
B	N	100	100	150
C		100	125	150
D		100	75	150
E		100	100	100
F		150	100	150

Table 4 summarizes the predicted versus average experimental results, where the mean predicted to average experimental load capacity was 0.94 ± 0.17, with coefficients of variation (COV) and determination (R2) of 18.34% and 0.71, respectively. The mean predicted to average experimental stiffness, calculated as per ASTM E2126–11 [7], was 1.36 ± 0.18, with coefficients of variation (COV) and determination (R2) of 13.17% and 0.89, respectively. A good agreement is evident between the FEM and experimental modes of failure (Fig. 2).

3. Parametric study

A preliminary analysis revealed that the support conditions significantly affect the nodes' stiffness and load capacity. Two cases of support conditions were compared, where the “Lab Support” condition is that used in the tests (Fig. 1b), whereas the “Full Contact” case simulated the conditions in practice where the glulam beams are supported over the whole corbel (Fig. 3a). As shown in Fig. 3b, the nodes with Full Contact case exhibited stiffer response but lower load-carrying capacity than those for Lab Support condition, which can be attributed to the rotational restraint and stress concentration at the corbel-column interface for the former case. Therefore, it was decided to use the full contact support conditions for the nodes in this parametric study.

Table 4: Validation of numerical models against the experimental results

Specimen ID	Peak load (kN)			Initial stiffness (kN/m)		
	P_{FEM}	P_{EXP}	P_{FEM}/P_{EXP}	K_{FEM}	K_{EXP}	K_{FEM}/K_{EXP}
A	65.8	78.0	0.84	149353	127123	1.17
B	68.2	81.3	0.84	162364	113006	1.44
C	97.2	95.4	1.02	267753	241878	1.11
D	42.2	43.7	0.96	104732	63606	1.65
E	97.4	76.5	1.30	268289	195135	1.37
F	102.6	92.3	0.74	256485	177392	1.45
Mean	_	_	0.95	_	_	1.36
SD	_	_	0.17	_	_	0.18
COV%	_	_	18.34	_	_	13.17
R^2	_	_	0.71	_	_	0.89

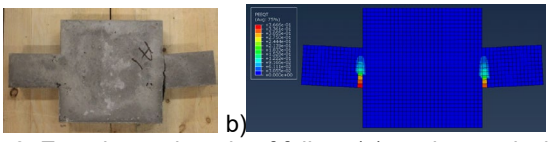

Fig 2: Experimental mode of failure (a); and numerical mode of failure (b).

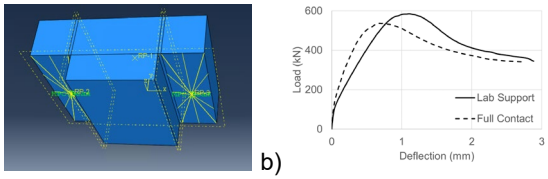

Fig 3: Full-contact support case (a); and load-deflection responses for different support conditions (b).

The parametric study included 32 FEMs, as listed in Tables 5 and 6. The investigated parameters were the shear span, depth, and width of the corbels, and CDP model parameters in tension and compression. It was decided to study the variation of each CDP parameter individually (i.e., while keeping all other variables the same as those in Table 2) to determine its impact on the response of the UHPC corbels. The ranges selected for each parameter were based on the available literature on UHPC [8].

It can be observed from Fig. 4 that the peak load and stiffness increased as the width or depth or shear span of the corbel decreased. It can also be observed that the post-peak branch declined more rapidly as the depth of the corbel increased beyond 175 mm or the shear span decreased. Generally, all FEMs failed in flexure at the corbel-column interface.

Changing the CDP parameters in compression did not significantly affect the load-deflection response of the nodes. An example is given in Fig. 5a where the variable is the peak compressive strength, f'_c. On the other hand, the variation of the tensile parameters of the CDP model exhibited remarkable influence on the response of those nodes (Fig. 5b, c), with the strength at rupture, $f_{t,r}$ being the most effective. For instance, increasing the rupture strength to 4 MPa resulted in exhibiting a nearly flat post-peak load-deflection response.

Table 5: Details of the FEMs of nodes to study the geometrical effects.

Specimen ID	a (mm)	h (mm)	a/h	b (mm)
X150-150-100	50	150	0.33	150
X150-150-150	75		0.5	
X150-150-200	100		0.67	
X150-100-150	75	100	0.75	
X150-200-150		200	0.38	
X150-250-150		250	0.3	
X200-150-150		150	0.5	200
X250-150-150				250
X300-150-150				300
X350-150-150				350
X400-150-150				400
X500-150-150				500

Table 6: Details of the FEMs of nodes with different strength model parameters.

Specimen ID	Variable	Value
X300-150-150-1	f_c (MPa)	75
X300-150-150-2		100
X300-150-150-3	f'_c (MPa)	110
X300-150-150-4		150
X300-150-150-5	$f_{c,crush}$ (MPa)	20
X300-150-150-6		60
X300-150-150-7	$\varepsilon_{pl,peak}$	0.002
X300-150-150-8		0.004
X300-150-150-9	$\varepsilon_{pl,crush}$	0.01
X300-150-150-10		0.03
X300-150-150-11	$f_{t,cr}$ (MPa)	0.4
X300-150-150-12		1.0
X300-150-150-13	f_t (MPa)	7.0
X300-150-150-14		11.0
X300-150-150-15	$f_{t,r}$ (MPa)	0.5
X300-150-150-16		4.0
X300-150-150-17	$\varepsilon_{pl,t}$	0.002
X300-150-150-18		0.005
X300-150-150-19	$\varepsilon_{pl,r}$	0.02
X300-150-150-20		0.04

4. Analytical model

The load-carrying capacities of the FEMs in this parametric study were calculated assuming the corbels to act as prisms tested under four-point bending and using the experimentally determined flexural strength for the used UHPC mix as follows.

$$P_{flex} = \frac{fbh^2}{3a} \quad (1)$$

where P_{flex} is the predicted load, f is the flexural strength, b and h are the average width and depth of the specimen at the fracture, respectively, and a = the shear span. From Table 7, it can be observed that the mean predicted-to-FEM ratio for the load capacity of 1.44 ± 0.14, with coefficients of variation (COV) and determination (R^2) of 9.6% and 0.96, respectively. Therefore, a regression analysis was performed for the results of the FEMs where each variable (i.e., corbel width, depth and shear span, and tensile strength of UHPFRC) was individually isolated and analyzed against the normalized predicted load capacity of the node. In addition, the direct tensile strength was used in lieu of the flexural strength.

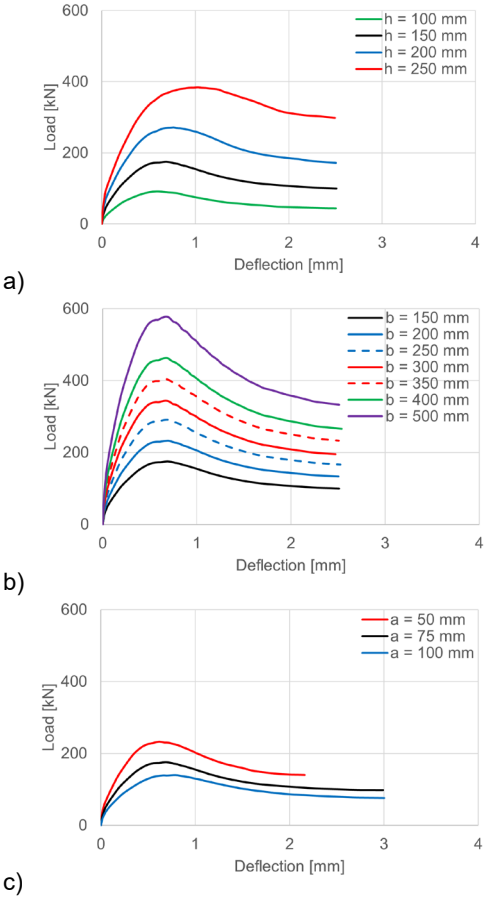

Fig 4: Load-deflection responses for the nodes with various corbel: depths (a); widths (b); and shear spans (c).

Consequently, the load prediction equation is modified as follows.

$$P_{flex,pro} = \frac{4.9 f_t^{0.7} bh^{1.6}}{3a^{0.7}} \quad (2)$$

where f_t is the ultimate direct tensile strength of the used UHPFRC. The results of load predictions using Eq. (2) resulted in a mean predicted-to-FEM load capacity of 1.00 ± 0.02, with coefficients of variation (COV) and determination (R^2) of 2.3% and 0.997, respectively. When applied to the experimental results, Eq. (2) resulted in a mean predicted-to-EXP load capacity of 0.88 ± 0.1, with coefficients (COV) and (R^2) of 12.1% and 0.78, respectively, which was deemed satisfactory given the scatter of the test results.

5. Conclusions and outlook

The following conclusions can be drawn:

Table 7: Details of the analytical results for the FEMs of nodes without bars.

Specimen ID	P_{FEM}	P_{flex}	P_{flex}/P_{FEM}	$P_{flex,pro}$	$P_{flex,pro}/P_{FEM}$
X150-150-100	232.3	364.5	1.57	228.9	0.99
X150-150-150	175.3	243	1.39	172.3	0.98
X150-150-200	139.7	182.3	1.30	140.9	1.01
X150-100-150	91.8	108	1.18	90.1	0.98
X150-200-150	271.0	432	1.59	273.0	1.01
X150-250-150	384.2	675	1.76	390.1	1.02
X200-150-150	232.7	324	1.39	229.7	0.99
X250-150-150	290.4	405	1.39	287.2	0.99
X300-150-150-13	275.8	365.8	1.33	282.5	1.02
X300-150-150	323.4	486	1.50	344.6	1.07
X300-150-150-14	376.3	574.8	1.53	387.6	1.03
X350-150-150	404.1	567	1.40	402.1	0.99
X400-150-150	462.1	648	1.40	459.5	0.99
X500-150-150	578.2	810	1.40	574.4	0.99
Mean			1.44		1.00
SD			0.14		0.02
COV%			9.6		2.3
R^2			0.96		0.997

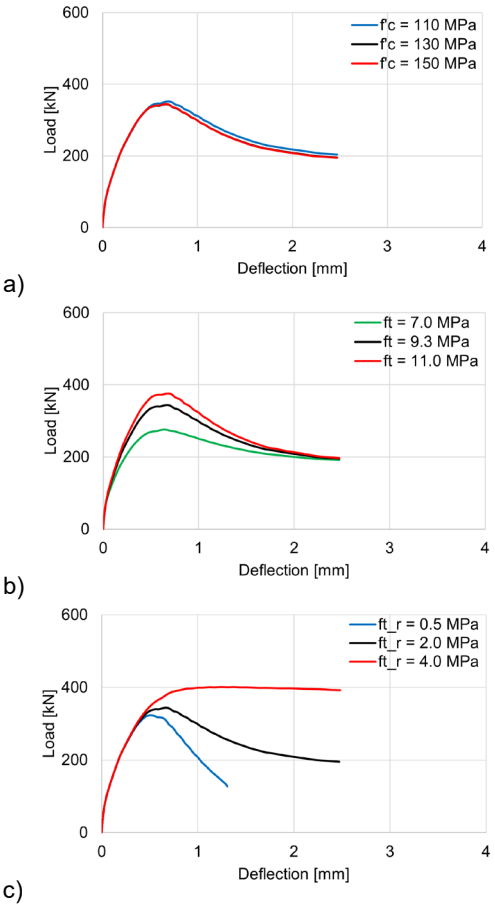

Fig 5: Examples of load-deflection responses for the nodes with various: compressive strengths (a); peak tensile strengths (b); and tensile strengths at rupture (c).

- A uniform load distribution at supported glulam beams is both a more accurate representation of the applied node. It represents the more critical load case over the lab-tested load case.
- The effects of UHPC corbel geometry do not follow the conventional flexural strength equation for concrete prisms. Based on the numerical results, a modified prediction equation is provided.
- Increasing the concrete compressive strength of UHPC had an insignificant effect on the load-deflection response of the nodes.
- Changing the CDP parameters for UHPC in tension remarkably influences the load carrying capacity and the post-peak behaviour, especially the tensile strength at peak and rupture.

It is recommended that the developed analytical model is checked using actual UHPC mixtures with different properties in compression and tension. Wider ranges of geometry are also required to extend the validity of the proposed model.

Acknowledgements

This research was supported by the Mitacs Accelerate Fellowship and the financial support provided by Fast + Epp Structural Engineers Ltd.

References

[1] Mulder, M., Dickof, C., Jackson, R., Kim, J. (2023). Case Study: A HIGH-RISE TIMBER BRACED AND CLT SHEARWALL BUILDING IN VANCOUVER, BRITISH COLUMBIA. Canadian Conference - Pacific Conference on Earthquake Engineering 2023, Vancouver, British Columbia.

[2] Abdallah, A. Shahnewaz, M., Dickof, C., Tobber, L. Production of UHPFRC nodes for timber structures in the Canadian West Coast: Lessons learned. Canadian Society for Civil Engineering (CSCE) Conference, Niagara Falls, ON, Canada (forthcoming).

[3] Lubliner, J., Oliver, J., Oller, S., Onate, E. (1989). A plastic-damage model for concrete. Int. J. Solids Struct., 25(3), 299–326.

[4] Kang, S. T., Lee, Y., Park, Y. D., Kim, J. K. (2010). Tensile fracture properties of an Ultra High Performance Fiber Reinforced Concrete (UHPFRC) with steel fiber. Composite structures, 92(1), 61-71.

[5] Ridha, M. M., Al-Shafi'i, N. T., Hasan, M. M. (2017). Ultra-high performance steel fibers concrete corbels: Experimental investigation. Case studies in construction materials, 7, 180-190.

[6] Shafieifar, M., Farzad, M., Azizinamini, A. (2017). Experimental and numerical study on mechanical properties of Ultra High Performance Concrete (UHPC). Construction and Building Materials, 156, 402-411.

[7] ASTM E2126-11. Standard test method for cyclic (reversed) load test for shear resistance of vertical elements of the lateral force resisting systems for buildings. American Society for Testing Materials (ASTM) International, West Conshohocken, PA (2011).

[8] Bahij, S., Adekunle, S. K., Al-Osta, M., Ahmad, S., Al-Dulaijan, S. U., Rahman, M. K. (2018). Numerical investigation of the shear behavior of reinforced ultra-high-performance concrete beams. Structural Concrete, 19, 305–317.